

# **SATELLITE IMAGERY ELABORATION (ASTER SENSOR, TERRA SATELLITE), IN ORDER TO MAP ROCK DISTRIBUTION IN EXTREME AREAS. THE PRINCE ALBERT MOUNTAIN CHAIN (VICTORIA LAND - ANTARTICA).**

A. Favretto\* R. Geletti\*\*

\*Dept. Of Geographical and Historical Sciences University of Trieste (Italy) andrea.favretto@dsgs.univ.trieste.it

\*\*Istituto nazionale di Oceanografia e Geofisica sperimentale Trieste (Italy) rieletti@ogs.it

**KEY WORDS:** Geology, Identification, Global Environmental Databases, Satellite, Thematic, Method.

## **ABSTRACT.**

The present paper is a first attempt to use Remote Sensing and GIS methodologies in order to draw a rock distribution map in a extreme land as Antarctica.

To this aim we elaborated an ASTER sensor image (Terra satellite). This sensor records medium resolution satellite images (from 15 m to 90 m pixels) in 14 different bands (from visible to thermal infrared). In the scientific community ASTER data represent a new tool in order to create land use maps, thermal distribution maps and 3d models of the territory.

The adopted methodology is applied to a training area in Prince Albert mountain chain (Trans Antarctica Ridge – Victoria Land – Antarctica).

We checked the spectral response of the satellite image pixels; then we estimated the kind of rock by the presence of different minerals in it. We did this comparing the reflectance values of the satellite image pixels with the one recorded in laboratory on each mineral in the different wavelengths corresponding to the ASTER sensor 14 bands.

In order to control our estimation, we used a geologic map of the same area. This one was drawn within the framework of the Italian National Research Program in Antarctica (PNRA).

We choose a ASTER sensor satellite scene recorded in the period of maximum ice cover on the land, in order to grant a minimum outcrop in the case of an eventual manual check in Antarctica.

## **1. Introduction**

This work is aimed at developing a methodology to allow the mapping of extreme geographical areas like Antarctica. The methodology consists of using remote sensing combined with GIS techniques and has been developed in order to support traditional *in situ* field survey techniques.

The Antarctic continent is a deserted and remote landmass, almost entirely covered with ice. It has a complex geological history, which has not yet been fully understood or rebuilt and it is still in evolution. Since ice occupies more than 98% of the entire continent, fieldwork and surveys involving traditional methods of investigation by direct observation of outcrops or sediments is possible only in a few areas: where the ice is absent, along mountain chains or on top of isolated peaks and under the peri-Antarctic seas. Our work shows how combining information obtained by remote sensing with the ones given by direct outcrop observation can improve the geological history knowledge of the Antarctic continent. The study area is located in the Prince Albert mountain chain which belongs to the Transantarctic Mountains (TM). TM lie on the cost of the Victoria Land (VL), western Ross Sea, and they extend for more than 4500 km, reaching an altitude of about 4000 m. The TM are one of the world's best examples of rift shoulders (Stern, Brink, 1989; Fitzgerald, 1992). Geological information about the extension of the West Ross Sea region comes primarily from fieldwork carried out along the TM. The study area is characterized by outcrops of Precambrian—Paleozoic crystalline (granitic) basement and Jurassic volcanic sills (Gunn, Warren, 1962; Elliot, 1975). This area has been chosen as it presents the best conditions for this study, having a good coverage of mapped outcrops (Capponi et al., 1999), and thus allowing us to verify the results obtained from application of the methodology we propose.

The methodology has been tested on an image obtained from the satellite Terra, ASTER sensor (1) dated 1/11/2000. The image has been acquired during the Antarctic winter in order to have the most ice sheet coverage. This fact allows us to study the outcrop and thus, to test the methodology in the worst ice conditions. The methodology consists of comparing the pixel spectral responses of the studied satellite image acquired by ASTER at different bandwidths with the reflectance values obtained from different wavelengths recorded on the mineral in laboratory. Two different rock types have been identified and mapped. The results have been compared with the geological map of the area (Capponi et al., 1999) compiled in the context of the Programma Nazionale di Ricerche in Antartide (PNRA). This comparison allowed a first testing of the used methodology.

## **2. Database**

We used the following data:

- An ASTER sensor scene (Terra satellite), dated 1/11/2000;
- A geological map: Relief Inlet Quadrangle (Victoria Land), 1:250.000 scale.

All data elaboration have been made with Erdas Immagine 8.6 and Esri Arc Gis 8.2

## **3. Data elaboration**

We first transformed the PNRA geologic map in a digital form. The digital map has been then rectified in the Polar Stereographic coordinate system (WGS 84 spheroid). With a subset procedure we isolated the study area (Prince Albert Mountain, area around the Larsen Glacier, fig. 1).

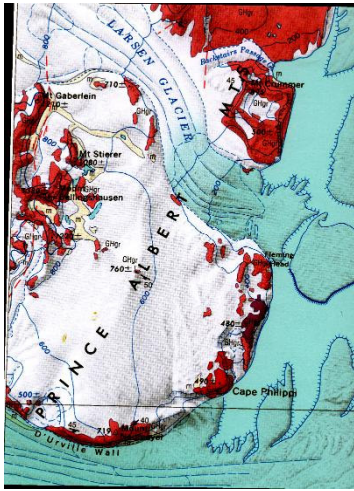


Figure 1. *Geologic map (Capponi et al., 1999) of the study area Prince Albert Mountain, around the Larsen Glacier (the digital map has been rectified in the Polar Stereographic coordinate system WGS 84 spheroid).*

We imported the 1/11/2000 ASTER sensor scene in the Erdas Imagine format and we rectified it in the Stereo Polar coordinate system. We isolated the study area with another subset procedure. Fig. 2 shows the ASTER scene in false colour composition (red channel: near infrared; green channel: red; blue channel: green).

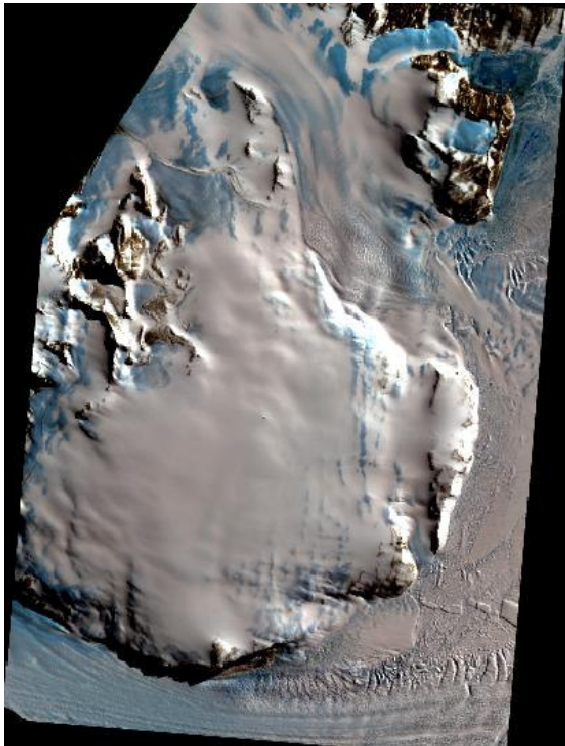


Figure 2. *The ASTER scene (1/11/2000 ASTER sensor) in false colour composition (red channel: near infrared; green channel: red; blue channel: green); this subset of the study zone has been rectified in the Stereo Polar coordinate system.*

Observing fig. 2 you can see clearly the wide icy cover on the land: the isolated rock outcrops are in fact concentrated in the Mount Crummer area (North of the Larsen Glacier). You can

see other rock outcrops in the Stierer and Bellinghansen Mountains area, at the East of Philippi Cape. Other rock outcrops are visible on the South part of the image, near Urville Wall.

Observing again the fig. 1, you can see that in the study there are two principal kinds of composite rocks. These are: Granite Harbour Granodiorite and Granite (GHGr); Granite Harbour Gabbro and Ultramafite (GHGa). GHGr rocks are painted in pink while GHGa in violet. GHGr areas are very diffuse on the land, GHGa areas are instead concentrated in a small area, close to the North side of Philippi Cape. The two rocks are characterized by the presence of several particular minerals, we choose among them the Biotite and the Serpentine in order to recognize the type of rock on the basis of the presence of the mineral in it. The rock outcrops with high biotite concentration (and low Serpentine) belong to the granite GHGr complex, while rock outcrops with high serpentine concentrations (and low Biotite) belong to the granite GHGa complex.

In order to discriminate the two granite complexes, we used the Jet Propulsion Laboratory (JPL) spectral libraries (2). In fig. 3 are drawn the spectral responses of the Serpentine (light blue) and the Biotite (yellow) in the different wavelengths recorded by the ASTER sensor bands. The grain particulate is the bigger one (125-500  $\mu\text{m}$ ). We choose this grain size because it is the one that gave the best results in our analysis.

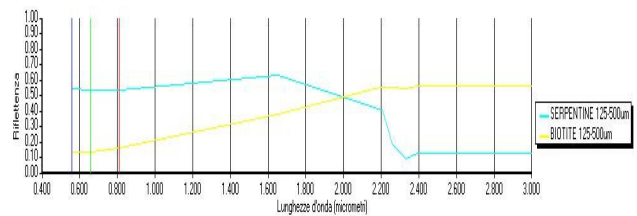


Figure 3. *Spectral responses of the Serpentine (light blue) and the Biotite (yellow). It is used the Jet Propulsion Laboratory (JPL) spectral libraries.*

On the horizontal axis is measured the wavelength ( $\mu\text{m}$ ). On the vertical axis is measured the relative reflectance normalized to one. If we check table 1, which has some ASTER sensor information (spectral, spatial, radiometric resolution of each band in the sensor subsystem: visible – VNIR, middle infrared – SWIR, thermal infrared – TIR), we can realize that the laboratory measurements are fit in the sensor features.

System	Band	Spectral Range	Spatial Resolution	Radiometric Resolution
VNIR	1	0.52-0.60	15 m	8 bit
	2	0.63-0.69		
	3	0.78-0.86		
SWIR	4	1.60-1.70	30 m	8 bit
	5	2.145-2.185		
	6	2.185-2.225		
	7	2.235-2.285		
	8	2.295-2.365		
	9	2.360-2.430		
TIR	10	8.125-8.475	90 m	12 bit
	11	8.475-8.825		
	12	8.925-9.275		
	13	10.25-10.95		
	14	10.95-11.65		

Table 1. *Aster main characters. Modified by: "Aster User Handbook, vers. 2" (Abrams and others, 2003).*

The graphs in fact begin from 0.52  $\mu\text{m}$  value; three bars are also visible in correspondence of the first three ASTER bands (green, red and near infrared), which report the used channel in the false colour composition of fig. 2. We decided to stop the reflectance values at 3  $\mu\text{m}$  because after 2.4  $\mu\text{m}$  the y value is constant in both cases (Biotite and Serpentine). As you can see from the graphs, the minerals have two different laboratory behaviours. The Serpentine has high reflectance values at low wavelengths. Then reflectance values begin to low after 1.6  $\mu\text{m}$ , they fall after 2.3  $\mu\text{m}$  and then they remain constant from 2.4  $\mu\text{m}$ . The Biotite instead has low reflectance values at low wavelengths, then it has a growing almost linear trend till 2.2  $\mu\text{m}$ , when it begins to register a constant reflectance value.

On the basis of the laboratory spectral response behaviours, we tried to discriminate GHGr and GHGa rock complexes in the outcrops of the study area. This discrimination has been realized on the basis of the presence/absence of the Biotite and the Serpentine minerals. The Biotite presence may point out the GHGr rock composite presence in the study area while the Serpentine presence may point out the GHGa rock composite. In order to classify the ASTER sensor we applied the Constrained Energy Minimization algorithm (CEM). CEM algorithm produces a thematic layer with pixel that can assume a value from 0 to 1. If the pixel value is close to 1, there is a close similarity between laboratory and land spectral response; if the pixel value is close to 0, the contrary. We applied CEM algorithm twice: one for the Biotite and one for the Serpentine. Fig. 4 shows CEM estimated Biotite concentrations: white pixels have high values while dark pixels, low values. In fig. 4a you can see the absolute frequencies histogram of fig. 4. Fig. 5 shows CEM estimated Serpentine concentrations. Fig. 5a shows the absolute frequencies histogram of fig. 5.

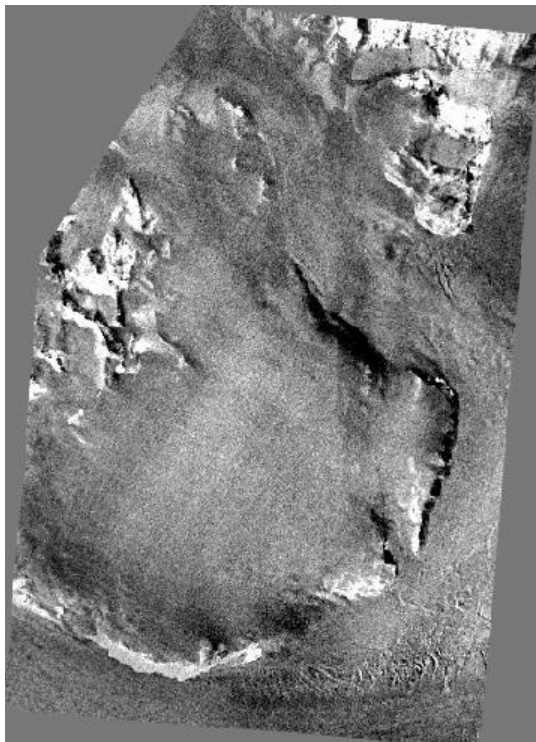


Figure 4. CEM estimated Biotite concentrations: white pixels have high values while dark pixels, low values.

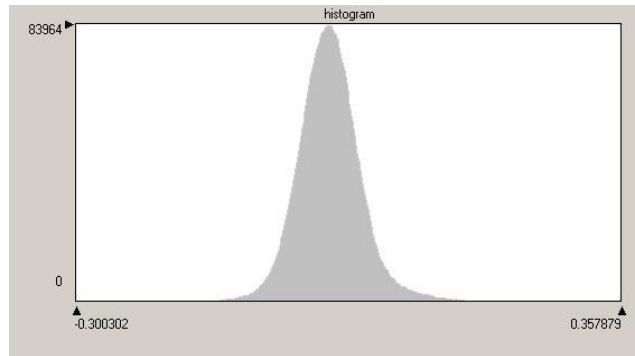


Figure 4a. The figure shows the absolute frequencies histogram of fig. 4.

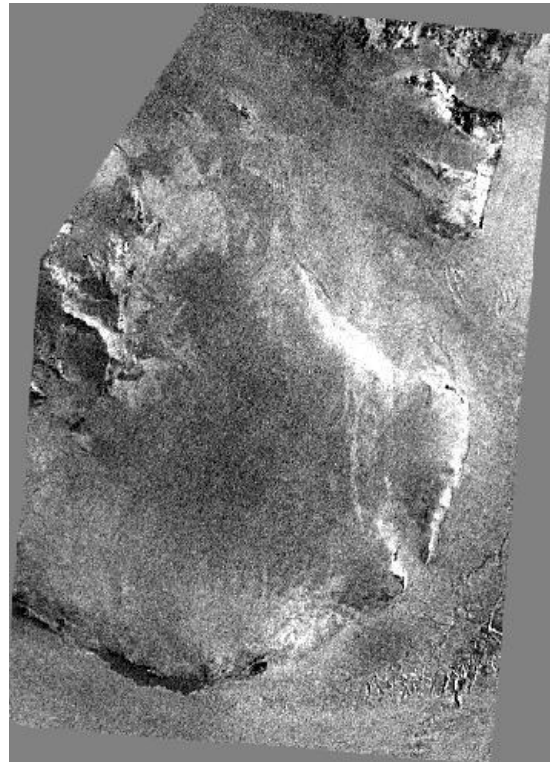


Figure 5. CEM estimated Serpentine concentrations: white pixels have high values while dark pixels, low values.

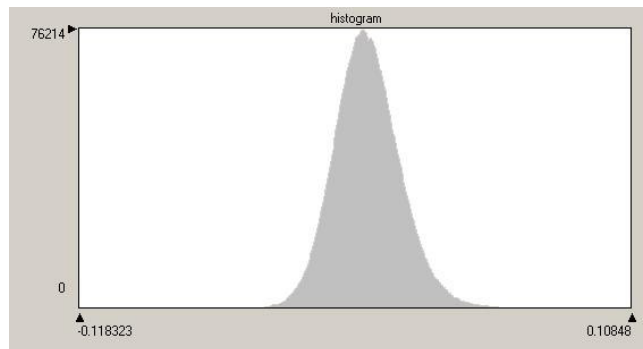


Figure 5a. The figure shows the absolute frequencies histogram of fig. 5.

We give also the following statistical information about the two CEM thematic layers:

- Biotite (fig. 4). Min value: -0.3; max. value: +0.357; mean: 0.005; st. dev.: 0.041.



- Serpentine (fig. 5). Min value: -0.12; max. value: +0.11; mean: 0; st. dev.: 0.014.

Observing fig. 4a and 5a and considering the given statistical information, we would like to say that:

- Biotite. Checking the pixel numbers of fig. 4 we found out that the pixels  $< 0$  are 1286080 over a whole of 3428880. We think to explain this error by the topographic features of the image (which caused some over lighting problems in the satellite scene). The normal distribution of the absolute frequencies (fig. 4a), suggests to classify the thematic layer in three classes. Medium class is built summing and subtracting from the mean value the st. dev. value ( $0.005 \pm 0.041$ ); high class is made by values  $\geq 0.046$ ; low class by values  $\leq -0.036$ . You can see the said classification in fig. 6.

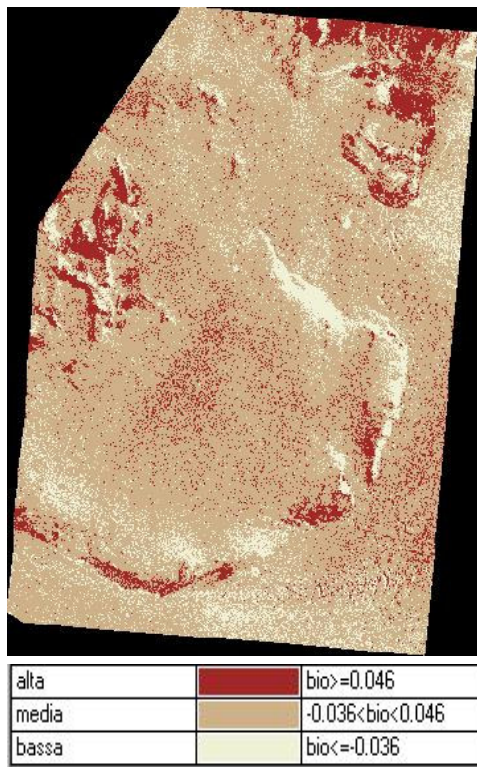


Figure 6. Three classification levels of the Biotite concentration (see text for more details)

We think that the high Biotite concentration areas could be enough correct while the low Biotite concentration areas may be not. We think that some pre processing procedures applied to the ASTER sensor image could correct the classification of the low concentration areas. These are: atmospheric and topographic corrections (which should low the errors caused by the morphology of the land – shadow areas, CEM pixels  $< 0$ ).

- Serpentine. Similarly to the Biotite case, the high number of pixel  $< 0$  (1478102 over a whole of 3428880) is also attributed to the light condition of the image (land morphology). We classified the image in three classes, using the same rules of the previous example (Biotite). Considering the mean and the st. dev. values (respectively 0 and -0.014) these are the three obtained ranges: low: serp.  $\leq -0.014$ ; medium: -

$0.014 < \text{serp.} < 0.014$ ; high: serp.  $\geq 0.014$ . You can see the said classification in fig. 7. As in the previous case, we think that the high Serpentine concentration areas are enough correct, while the low Serpentine concentration areas should be corrected with the said pre processing procedures.

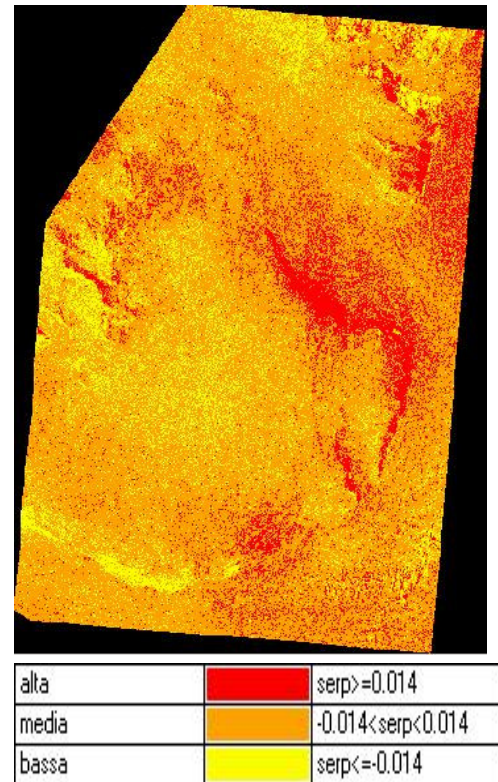


Figure 7. Three classification levels of the Serpentine concentration (see text for more details).

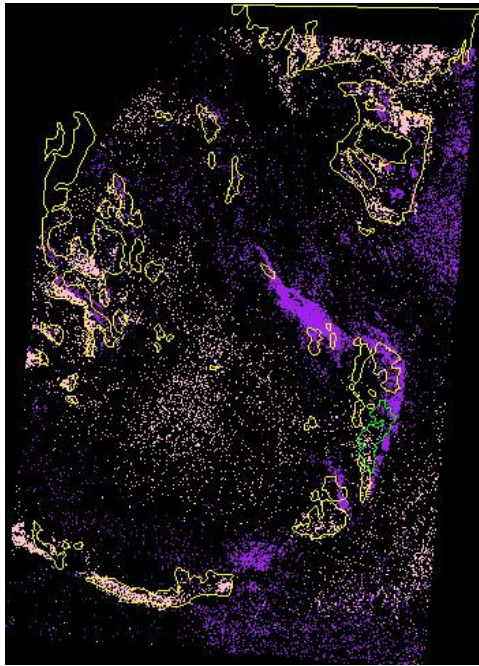
#### 4. Results and conclusions

At last we ran the so called “Matrix” procedure. This procedure overlays the thematic layers of fig. 6 and 7 (Biotite and Serpentine concentrations by the CEM algorithm) in order to point out all the possible combinations among the classes. Fig. 8 shows in pink the high Biotite and low Serpentine areas; in violet are drawn instead the low Biotite and high Serpentine areas.

In order to make a first classification check, we overlaid on the pink and the violet areas two vector layers, which were drawn on the basis of the PNRA map. The yellow vector layer shows the Biotite areas (GHGr), while the green one, the Serpentine areas (GHGa).

We would like to note that:

- Especially in the case of the low mineral concentrations, we think that the pink and violet areas may be overestimated. This fact may have happened because of shadow zones existence in the raw data satellite scene. In fact we saw that the CEM algorithm tends to consider the shadow zones as mineral low concentration ones.
- In the case of the isolated pixel existence inside the icy areas, we think that these pixels may show morenic settlements instead of emerged rocks. We intend at this aim to refine our classification on the basis of this hypothesis.



alta bio-alta serp	
alta bio-media serp	
alta bio-bassa serp	
media bio-alta serp	
media bio-media serp	
media bio-bassa serp	
bassa bio-alta serp	
bassa bio-media serp	
bassa bio-alta serp	

Figure 8. The image shows in pink the high Biotite and low Serpentine areas; in violet are drawn instead the low Biotite and high Serpentine areas. In order to make a first classification check, we overlaid on the pink and the violet areas two vector layers, which were drawn on the basis of the PNRA map. The yellow vector layer shows the Biotite areas (GHGr), while the green one, the Serpentine areas (GHGa).

Looking at the fig. 8 vector and raster layer overlays, we think that our first try to map the Antarctica geological areas by means of the Remote Sensing techniques has been useful. In fact the realized classification seems to be in accord with the local sampling drawn (PNRA map). This good result is visible in the Mount Crummer area (Biotite GHGr areas, North-East of the satellite scene). In this area is evident a good overlay between the estimated Biotite concentration and the local sampling. The South-East area of the image shows instead some bigger problems. In this area in fact the shadows/light conditions of some spots may have caused some errors in the CEM algorithm classification.

In the future, we intend to develop our method with the following enhancements:

- The atmospheric and topographic correction of the ASTER sensor scene (by the building of a Digital Terrain Model of the study area. These corrections should help to solve under and over lighting problems of the raw data.
- Operate a more accurate classification of the rock outcrops in the ASTER sensor scene. In fact the PNRA map has been drawn on the basis of summer samplings while the satellite scene is dated November, a local very cold period. This fact has surely caused a different ice cover in the two different maps.

After the said corrections we will verify the rock classification on the basis of automated procedures that can count the pixel numbers in the PNRA map and in the classified satellite image. At last we will analyse the study area with a different year satellite image in order to point out some possible icy cover changes and, in this way, make a better rock outcrop classification.

## Notes

(1) Terra satellite has been launched in December 1999 by NASA within the framework of EOS project (Earth Observing System). It carries the following instruments: ASTER (Advanced Spaceborne Thermal Emission and Reflection Radiometer);

CERES (Clouds and the Earth's Radiant Energy System); MISR (Multi-angle Imaging Spectro-Radiometer);

MODIS (Moderate-resolution Imaging Spectroradiometer); MOPITT (Measurements of Pollution in the Troposphere).

ASTER acquire high resolution Earth images (pixel from 15 to 90) in 14 different bands of electro-magnetic spectrum, from visible to thermal infrared (Abrams et al. 2003). In the scientific community, ASTER images can be considered a very innovative tool to obtain detailed maps of land surface temperature, emissivity, reflectance and elevation.

(2) The JPL Spectral Library includes laboratory reflectance spectra of 160 minerals in digital form. Data for 135 of the minerals are presented at three different grain sizes: 125-500 $\mu$ m, 45-125 $\mu$ m, and <45 $\mu$ m.

(3) The Constrained Energy Minimization (CEM) algorithm attempts to maximize the response of

a target spectrum and suppress the response of the unknown background signature(s). It is appropriate to the situation where the sought material is a minor component of the scene. It is optimal for detection of distributed subpixel targets such as mineral occurrences or sparse vegetation (ERDAS, 2002).

(4) Calculated abundance values can be negative or greater than one. The negative values are a result of statistical variations around the assumption of distributed noise with a zero mean (maybe connected to the atmospheric scattering or to under/over lighting conditions due to the land morphology). Abundances greater than one can result if the input target spectrum is not entirely pure or of exactly the same composition as pixels within the image (ERDAS, 2002).

(5) Matrix analysis produces a thematic layer that contains a separate class for every coincidence of classes in two layers. In other words, it gives all the possible combinations of the classes of the thematic layers (3 classes for the Biotite and 3 classes for the Serpentine = 9 classes in the matrix layer).

## 5. References

- Abrams M., Hook S., Ramachandram B., *ASTER User Handbook*, Jet Propulsion Laboratory, Pasadena CA, EROS Data Center, Sioux Falls SD, 2003.
- Capponi G., Crespini L., Mecchieri M., Musumeci G., Pertusati P.C., *Relief Inlet Quadrangle (Victoria Land) – Antarctic Geological 1:250.000 Map Series*; PNRA (Programma Nazionale di Ricerche in Antartide), University of Siena, 1999.
- Elliot, D. H., *Tectonics of Antarctica – A review*, Am. J. Sci., 275°, 45-106, 1975.
- ERDAS, *Imagine Spectral Analysis User's Guide*, Erdas Inc. Leoca Geosystem, GIS & Mapping Division, Atlanta, 2002.
- Fitzgerald, P. G., *The Transantarctic Mountains of Southern Victoria Land: the application of apatite fission track analysis to a rift shoulder uplift*, Tectonics, 11, 634-662, 1992.

Gunn B. M. and Warren G., *Geology of Victoria Land between the Mawson and Mulock glaciers*, Antarctica, Bull. N.Z. Geol. Surv., 71, 1-157, 1962.

Stern T. A. and ten Brink U. S., *Flexural uplift of the Transantarctic Mountains*, J. Geophys. Res., 94, 10315-10330, 1989.

## 6. Acknowledgements

We would like to thank EOS Data gateway center (Earth Observing System, NASA) for having supplied us the Aster sensor image.

The Biotite and Serpentine charts were reproduced from the ASTER Spectral Library through the courtesy of the Jet Propulsion Laboratory, California Institute of Technology, Pasadena, California. Copyright © 1999, California Institute of Technology. ALL RIGHTS RESERVED.

## Tables

Table 1. Characteristics of the ASTER sensor System. Source: Aster User Handbook, vers. 2 – Abrams et al., 2003)

Subsystem	Band	Spectral range	Spatial resolution (m)	Radiometric resolution
VNIR	1	0.52-0.60	15	8 bit
	2	0.63-0.69		
	3	0.78-0.86		
SWIR	4	1.60-1.70	30	8 bit
	5	2.145-2.185		
	6	2.185-2.225		
	7	2.235-2.285		
	8	2.295-2.365		
	9	2.360-2.430		
TIR	10	8.125-8.475	90	12 bit
	11	8.475-8.825		
	12	8.925-9.275		
	13	10.25-10.95		
	14	10.95-11.65		

## Figure Captions

**Figure 1.** Geologic map (Capponi et al., 1999) of the study area Prince Albert Mountain, around the Larsen Glacier (the digital map has been rectified in the Polar Stereographic coordinate system, WGS 84 spheroid).

**Figure 2.** The ASTER sensor scene of 1/11/2000 in false colour composition (red channel: near infrared; green channel: red; blue channel: green) the image has been rectified in the Stereo Polar coordinate system (WGS 84 spheroid).

**Figure 3.** Spectral responses of the Serpentine (light blue) and the Biotite (yellow). The charts came from the Jet Propulsion Laboratory (JPL) spectral libraries.

**Figure 4.** CEM algorithm estimated Biotite concentrations: white pixels have high values while dark pixels, low values.

**Figure 4a.** Absolute frequencies histogram of the fig. 4 pixel values.

**Figure 5.** CEM algorithm estimated Serpentine concentrations: white pixels have high values while dark pixels, low values.

**Figure 5a.** Absolute frequencies histogram of the fig. 5 pixel values.

**Figure 6.** Three classification levels of the Biotite concentration (see text for more details)

**Figure 7.** Three classification levels of the Serpentine concentration (see text for more details)

**Figure 8.** The image shows in pink the high Biotite and low Serpentine areas; in violet are drawn instead the low Biotite and high Serpentine areas. In order to make a first classification check, we overlaid on the pink and the violet areas two vector layers, which were drawn on the basis of the PNRA map. The yellow vector layer shows the Biotite areas (GHGr), while the green one, the Serpentine areas (GHGa).